DALTON

Reactions of iridium and ruthenium complexes with organic azides†

Andreas A. Danopoulos,*‡[a] Robyn S. Hay-Motherwell,[b] (the late) Geoffrey Wilkinson, Sean M. Cafferkey,[c] Tracy K. N. Sweet[c] and Michael B. Hursthouse*[c]

[a] *Johnson Matthey Laboratory, Chemistry Department, Imperial College, London, UK SW7 2AY*
[b] *Christopher Ingold Laboratories, Department of Chemistry, University College London, 20 Gordon Street, London, UK WC1H 0AJ*
[c] *Department of Chemistry, University of Wales Cardiff, PO Box 912, Cardiff, UK CF1 3TB*

Interaction of N_3R with $Ir(mes)_3$ (mes = mesityl, $C_6H_2Me_3$-2,4,6) gave products dependent on the nature of the azide. When R = mes, the tetrazenido amide complex **1** is obtained in which dehydrogenative coupling of the mesityl groups *via* the *o*-methyls has occurred; thermolysis of **1** in toluene resulted in cleavage of the tetrazene ring and formation of amide complex **2**. When R = Ph, the aryl tetrazenido amide complex **3** is formed. Photolysis of a mixture of $N_3(mes)$ and $[RuCl_2(PPh_3)_3]$ followed by phosphine exchange gave the tetrazene complex $[Ru^{II}Cl_2\{N_4(mes)_2\}(PMe_3)_2]$ **4**. Thermal reaction of $[RuCl_2H_2(PPr^i_3)_2]$ with $N_3(mes)$ gave the triazenophosphorane complex $[RuCl_3(PPr^i_3)\{N_3(mes)PPr^i_3\}]$ **5**. The ruthenium allyl amide $[Ru(PMe_3)_3\{NHC_6H_3Pr^i(\eta^3\text{-}CH_2CCH_2)\}]$ **6** bearing a new hybrid ligand was obtained by interaction of *trans*-$[RuCl_2(PMe_3)_4]$ with $Li[NH(C_6H_3Pr^i_2\text{-}2,6)]$ in di-*n*-butyl ether. Plausible reaction mechanisms accounting for the formation of the new compounds are proposed. Finally, the crystal structures of the complexes **1**–**6** have been determined. Complexes **1** and **2** have pseudo-square planar geometries involving the olefin formed by the coupled methyl groups of two mesityls and three (**1**) or two (**2**) amide nitrogens and a chlorine atom (**2**). Compound **3** has a trigonal bipyramidal metal centre with the axial Ir–N amide bonds longer than the equatorial ones; **4** has an octahedral structure with a bidentate tetragonal ligand and *trans* phosphines whilst **5** is distorted octahedral with a N,N-chelating phosphazide ligand. Complex **6** is also octahedral with the allyl groups occupying *cis* sites and the three Ru–P bonds in a *facial* arrangement.

Interest in the chemistry of the late transition-metal imido complexes stems from the belief that they may exhibit unusual reactivity towards a variety of substrates such as olefins, acetylenes and other small organic molecules.[1] Despite recent significant contributions in this area by several groups[2–4] the chemistry of iridium and ruthenium imido compounds is still underdeveloped.

In an effort to explore new methods for the synthesis of such species, we studied some reactions of aryl azides with readily oxidisable ruthenium and iridium compounds in the hope that this might constitute a simple route to imido complexes. Although imido complexes were not isolated, the products identified offer evidence for the involvement of metal–imido intermediates.

We also describe the preparation of a ruthenium complex bearing a new hybrid bidentate allyl amide ligand leading to the stabilisation of uncommon ruthenium–amide bonds.

Results and Discussion

Iridium and ruthenium tetrazene complexes

In order to investigate the accessibility of iridium imido complexes *via* oxidative routes using organic azides as imido group sources, we selected as starting material the $12e^-$ three-co-ordinate $Ir(mes)_3$ (mes = $C_6H_2Me_3$-2,4,6),[5] because it is easily and cleanly oxidised by oxygen or other oxo transfer reagents, such as Me_3NO, to $(mes)_3Ir^V{=}O$.[6] In addition, since compounds of type $Ir(mes)_4$[5] are known, a hypothetical $(mes)N{=}Ir(mes)_3$ would not exhibit unfavourable steric interactions. Other examples of Ir^V complexes are known or have been implicated in various reactions.[7]

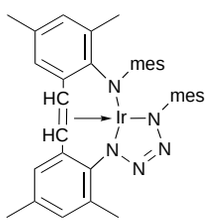

I

Interaction of an excess of $N_3(mes)$ with $Ir(mes)_3$ gave, after work-up an air stable blue paste as a dichloromethane solvate of **1**, which after crystallisation from ether gave blue crystals of **1**. Attempts to establish the identity of the compound by NMR spectroscopy were unsuccessful due to the complex and uninformative nature of the spectrum obtained. Therefore, an X-ray diffraction study was undertaken. The structural formula for the molecule is shown in structure **I** and a diagram from the crystal structure determination in Fig. 1; important bond lengths and angles are in Table 1.

The structure of compound **1** comprises an Ir metal centre in a pseudo-square planar environment, co-ordinated to the unusual tetradentate ligand by three amido N atoms and one olefin, the latter being assumed to occupy one site. The olefin is formally produced by dehydrogenative coupling and has a *trans* configuration. The bond lengths and angles within the ligand skeleton are consistent with the formulation shown in structure **I**. The Ir–N bond *trans* to the olefin site, Ir–N(1) is slightly longer than the other two, mutually *trans* Ir–N bonds [Ir–N(4), Ir–N(5)]. This may be due to a *trans* influence from the olefin bonding. The Ir–N_3o plane, where o is the midpoint of the olefin bond, is planar to within 0.08 Å. The C(23)–C(33) bond

† The work described herein was started, and several of the new compounds identified, before Sir Geoffrey's death last September. His co-authors dedicate this paper with deep respect and great affection to the lasting memory of a wonderful teacher, colleague and friend.

‡ *Present address*: Inorganic Chemistry Laboratory, University of Oxford, South Parks Road, Oxford, UK OX1 3QR.

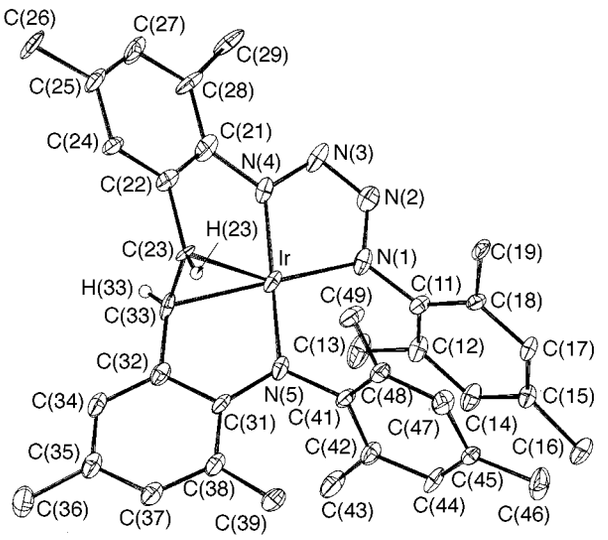

Fig. 1 The structure of compound **1**

Table 1 Bond lengths (Å) and angles (°) for compound **1**

Ir–N(1)	2.013(9)	Ir–C(23)	2.091(10)
Ir–N(4)	1.903(9)	Ir–C(33)	2.128(11)
Ir–N(5)	1.918(10)	N(1)–C(11)	1.423(14)
N(1)–N(2)	1.348(13)	N(4)–C(21)	1.460(14)
N(2)–N(3)	1.288(13)	N(5)–C(31)	1.418(14)
N(3)–N(4)	1.370(13)	N(5)–C(41)	1.452(13)
C(23)–C(33)	1.41(2)		
N(4)–Ir–N(1)	75.2(4)	N(2)–N(3)–N(4)	110.5(10)
N(4)–Ir–N(5)	173.7(4)	N(3)–N(2)–N(1)	117.4(9)
N(5)–Ir–N(1)	107.2(4)	N(2)–N(1)–Ir	114.9(7)
N(1)–Ir–C(23)	152.9(4)	N(3)–N(4)–Ir	121.8(7)
N(1)–Ir–C(33)	159.3(4)	N(2)–N(1)–C(11)	113.7(9)
N(4)–Ir–C(23)	82.0(4)	N(3)–N(4)–C(21)	116.7(9)
N(4)–Ir–C(33)	99.2(4)	C(11)–N(1)–Ir	131.0(8)
N(5)–Ir–C(23)	94.1(4)	C(21)–N(4)–Ir	120.3(7)
N(5)–Ir–C(33)	80.5(4)	C(31)–N(5)–Ir	120.3(7)
C(23)–Ir–C(33)	39.1(4)	C(41)–N(5)–Ir	122.5(7)
C(31)–N(5)–C(41)	117.0(9)		

makes an angle of 23.0° with this plane. The N–N distances in the tetrazenyl ligand, with the centre bond shorter than the two side bonds, are consistent with the formulation of the ligand as shown in structure **I**. The IrN_4 ring is planar to within 0.034 Å.

Compound **1** is thus a rare example of an amido complex of iridium(III). Its stability could be ascribed to the hybrid nature of the ligand, which in addition to the π donating amido groups has a π accepting olefinic site. The stability of another well characterised amido complex of iridium(III)[8] is also explained on a similar basis, *i.e.* the use of amido–phosphine hybrid ligands. Examples of Ir^{I} amides have been recently reported.[9]

The ^{1}H NMR spectrum of **1** reflects the lack of any symmetry elements in the molecule. All methyls attached to the aromatic rings are magnetically inequivalent. The complete assignment of the spectrum proved difficult. Although the mechanism of formation of **1** is self evidently complex a plausible sequence is discussed below in connection with compound **3**.

It is worthwhile mentioning that decomposition products of nitrene intermediates[10] are not observed in this reaction, indicating that free nitrenes are not involved in productive steps. Bulkier aryl azides, *e.g.* 2, 6-$Pr^{i}_2C_6H_3N_3$, or aryl azides with strongly electron withdrawing groups ($N_3C_6F_5$) known to be precursors of stable nitrenes[11] gave intractable mixtures after reaction with $Ir(mes)_3$. The reaction with N_3Ph is discussed below.

Compound **1** shows good thermal stability in the solid state indicating the reluctance of the tetrazene ring to undergo N_2 extrusion. Similar observations were previously made for cobalt,[12] rhodium, iridium[4a] and ruthenium[4a] tetrazene complexes.

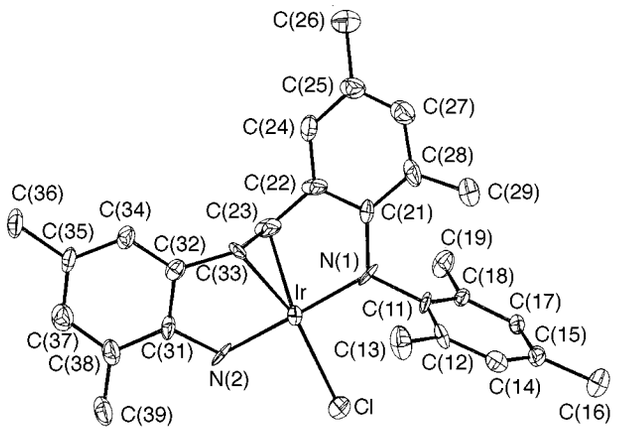

Fig. 2 The structure of compound **2**

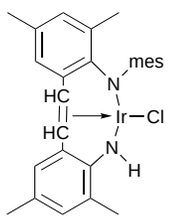

II

Table 2 Bond lengths (Å) and angles (°) for compound **2**

Ir–N(1)	1.939(6)	Ir–C(23)	2.091(7)
Ir–N(2)	1.914(6)	Ir–C(33)	2.097(6)
Ir–Cl	2.343(2)	N(1)–C(11)	1.444(7)
N(2)–C(31)	1.375(8)	N(1)–C(21)	1.426(8)
C(23)–C(33)	1.426(9)		
N(1)–Ir–C(23)	80.7(3)	N(2)–Ir–C(23)	98.7(3)
N(1)–Ir–C(33)	97.9(2)	N(2)–Ir–C(33)	80.5(2)
N(1)–Ir–Cl	94.9(2)	N(2)–Ir–N(1)	178.0(2)
N(2)–Ir–Cl	86.4(2)	C(33)–Ir–C(23)	39.8(2)
C(23)–Ir–Cl	157.5(2)	C(11)–N(1)–Ir	124.2(4)
C(33)–Ir–Cl	161.2(2)	C(21)–N(1)–Ir	117.7(4)
C(21)–N(1)–C(11)	117.5(6)	C(31)–N(2)–Ir	121.2(5)

Heating the previously mentioned solvate at 140 °C gives rise to compound **2**, shown in structure **II** and isolated in low to moderate yield after chromatographic work-up and crystallisation. A diagram of the molecule as determined by an X-ray diffraction study is given in Fig. 2; important bond lengths and angles are in Table 2. Its structure is related to that of **1**, with the common features in the diamidoalkene ligand showing very similar metric parameters. The IrN_2Clo group is planar to within 0.06 Å and the olefin bond makes an angle of 27.4° with this plane. The formal oxidation state for the Ir centre is also III.

In this unusual chemical transformation, which *formally* requires the loss of N_3(mes) from **1**, the only possible source of the chlorine atom is CH_2Cl_2. Homolytic pathways with possible electron transfer could be operating.

In order to gain more insight into the mechanism of formation of **1**, and in particular to trace the origin of each mesityl group in the final product, we studied the interaction of $Ir(mes)_3$ with N_3Ph. In this instance, due to the absence of the flanking *o*-methyl groups in the azide, the reaction followed a different pathway as witnessed by the product **3** isolated. Compound **3** was characterised by accurate mass spectroscopy (see Experimental section) and X-ray crystallography. Reliable analytical data could not be obtained possibly due to facile loss of dinitrogen or incomplete combustion even when a combustion catalyst was used. The structure of **3**, which is formally an Ir^{V} complex was determined by X-ray diffraction and is shown

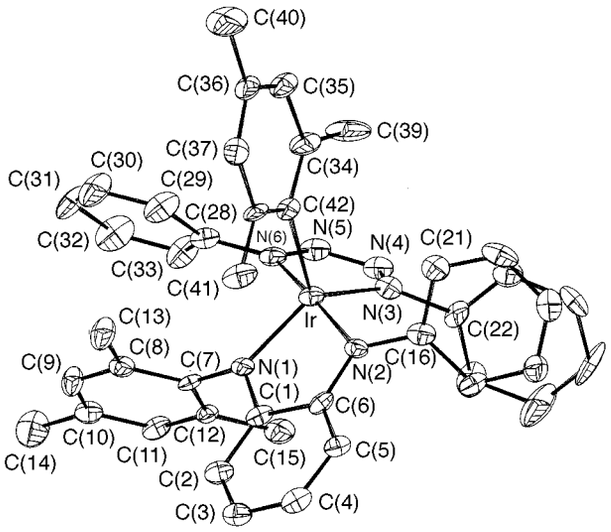

Fig. 3 The structure of compound **3**

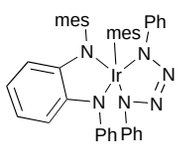

III

Table 3 Bond lengths (Å) and angles (°) for compound **3**

Ir–N(1)	1.975(5)	N(3)–N(4)	1.384(7)
Ir–N(2)	2.034(6)	N(4)–N(5)	1.314(8)
Ir–N(3)	1.928(6)	N(5)–N(6)	1.327(7)
Ir–N(6)	2.011(6)	N(1)–C(1)	1.372(8)
Ir–C(42)	2.110(6)	N(1)–C(7)	1.443(8)
N(2)–C(6)	1.352(8)	N(2)–C(16)	1.428(9)
N(3)–C(22)	1.445(8)	N(6)–C(28)	1.431(8)
N(1)–Ir–N(2)	79.0(2)	N(1)–Ir–C(42)	108.7(2)
N(1)–Ir–N(6)	99.4(2)	N(2)–Ir–C(42)	95.1(2)
N(3)–Ir–N(1)	135.7(2)	N(3)–Ir–C(42)	115.5(2)
N(3)–Ir–N(2)	99.2(2)	N(6)–Ir–C(42)	93.8(2)
N(3)–Ir–N(6)	75.6(2)	N(4)–N(5)–N(6)	115.3(5)
N(6)–Ir–N(2)	171.0(2)	N(5)–N(4)–N(3)	112.6(5)
N(4)–N(3)–Ir	118.9(4)	C(1)–N(1)–Ir	116.6(5)
N(5)–N(6)–Ir	117.0(4)	C(6)–N(2)–Ir	115.0(5)
C(1)–N(1)–C(7)	117.8(5)	C(7)–N(1)–Ir	112.0(4)
C(6)–N(2)–C(16)	119.4(6)	C(16)–N(2)–Ir	125.5(4)

schematically in structure **III**. A crystal structure diagram of the molecule is shown in Fig. 3; important bond lengths and angles are given in Table 3. The metal co-ordination is now slightly distorted trigonal bipyramidal, with the two chelating ligands each spanning one axial and one equatorial site. The IrN_4 ring has a shallow envelope configuration with the four N atoms planar to within 0.024 Å, and the Ir atom 0.15 Å out of the plane. The C_2N_2Ir ring is considerably buckled, with deviations of up to 0.5 Å. The axial Ir–N bonds [Ir–N(2), Ir–N(6)] are much lengthened and are longer than the equatorial one [Ir–N(3)], demonstrating the different π bonding capabilities of the axial and equatorial sites in Ir^{III} and Ir^{V} complexes. The Ir–C distance is very similar to that in compounds **1** and **2**. The tetraazenyl geometry is again consistent with the formulation shown, making it a formal 2 (−) ligand.

Plausible mechanisms for the formation of **1** and **3** are shown in Schemes 1 and 2, respectively. Initial interaction of an aryl azide with $Ir(mes)_3$ could lead to the formation of a transient arylimido trimesityl iridium which could rearrange to a mesityl imido iridium(III) complex [steps (*i*) and (*ii*)]. Alternatively, insertion of an aryl azide into the Ir–C bond leads directly to

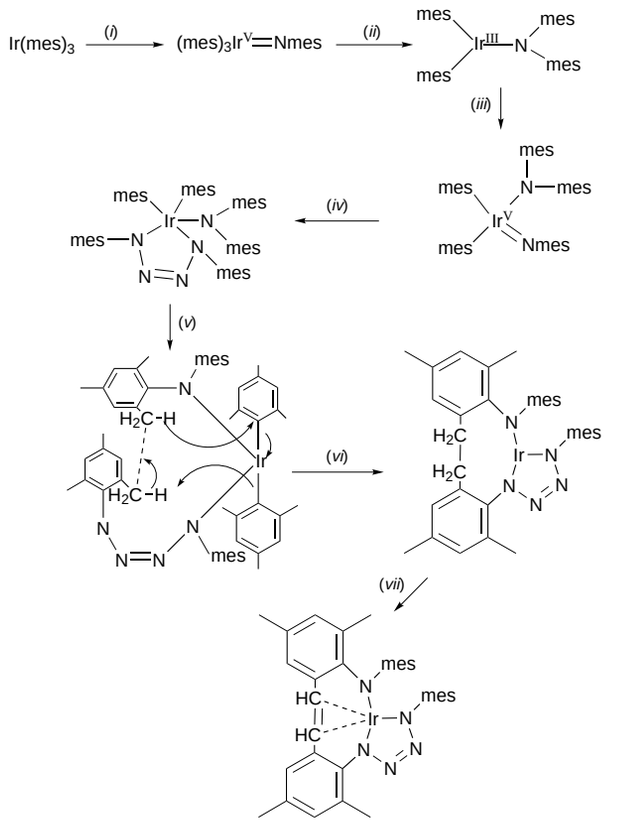

Scheme 1 Proposed mechanism for the formation of compound **1**: (*i*) N_3(mes), -N_2; (*ii*) rearrangement; (*iii*) oxidative addition; (*iv*) N_3(mes), cycloaddition; (*v*) intramolecular rearrangement; (*vi*) -2Hmes; (*vii*) -H_2

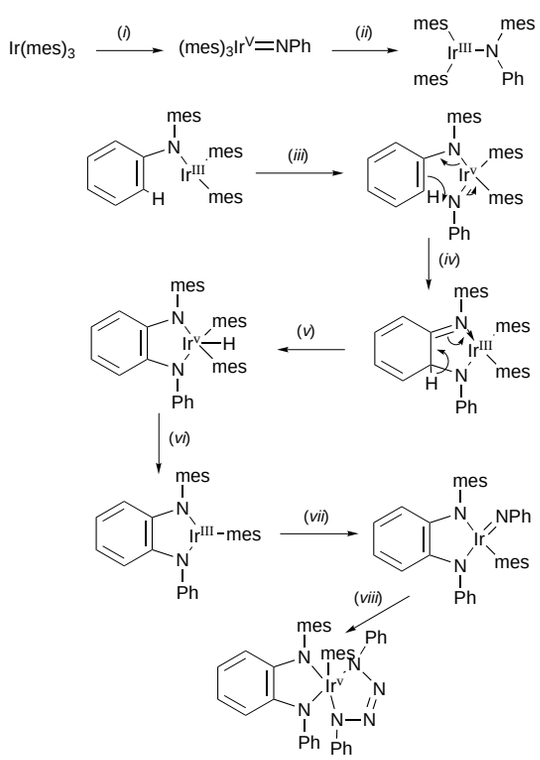

Scheme 2 Proposed mechanism for the formation of compound **3**: (*i*) N_3Ph, -N_2; (*ii*) rearrangement; (*iii*) N_3Ph, -N_2; (*iv*) rearrangement; (*v*) transfer of *o*-H; (*vi*) -Hmes; (*vii*) N_3Ph, -N_2; (*viii*) N_3Ph, -N_2

the intermediate $(mes)_2IrNR(mes)$ (R = aryl) for an analogous nickel reaction, see ref. 13. After this step the proposed reaction pathways diverge, the nature of the product depending on the presence or absence of the crucial *o*-methyl groups in the aromatic ring (R) of the reacting azide.

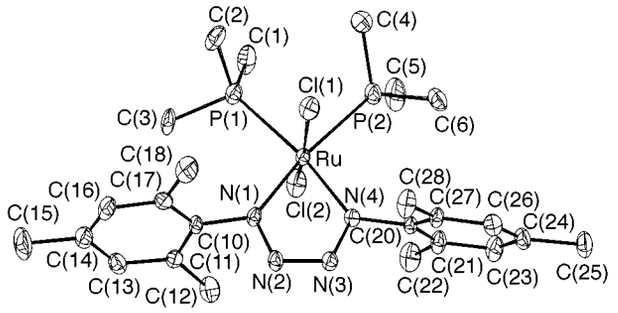

Fig. 4 The structure of compound **4**

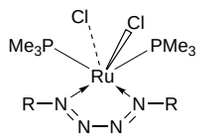

IV

Table 4 Bond lengths (Å) and angles (°) for compound **4**

Ru–N(1)	2.022(3)	P(1)–C(1)	1.817(5)
Ru–N(4)	2.033(3)	P(1)–C(2)	1.806(5)
Ru–Cl(1)	2.3636(11)	P(1)–C(3)	1.799(4)
Ru–Cl(2)	2.3655(12)	P(2)–C(4)	1.807(5)
Ru–P(1)	2.4194(12)	P(2)–C(5)	1.809(5)
Ru–P(2)	2.3988(13)	P(2)–C(6)	1.837(5)
N(1)–N(2)	1.307(4)	N(1)–C(10)	1.448(5)
N(2)–N(3)	1.338(4)	N(4)–C(20)	1.454(5)
N(3)–N(4)	1.313(4)		
N(1)–Ru–N(4)	73.22(13)	Cl(1)–Ru–Cl(2)	165.65(4)
P(2)–Ru–P(1)	91.10(4)	N(1)–Ru–P(1)	98.20(9)
N(1)–Ru–Cl(1)	97.71(9)	N(1)–Ru–P(2)	170.57(10)
N(1)–Ru–Cl(2)	93.68(9)	N(4)–Ru–P(1)	171.31(10)
N(4)–Ru–Cl(1)	93.38(9)	N(4)–Ru–P(2)	97.52(10)
N(4)–Ru–Cl(2)	98.25(9)	C(1)–P(1)–Ru	115.6(2)
Cl(1)–Ru–P(1)	89.07(4)	C(2)–P(1)–Ru	118.2(2)
Cl(1)–Ru–P(2)	80.75(4)	C(3)–P(1)–Ru	117.1(2)
Cl(2)–Ru–P(1)	80.67(4)	C(4)–P(2)–Ru	118.1(2)
Cl(2)–Ru–P(2)	89.39(4)	C(5)–P(2)–Ru	116.9(2)
C(2)–P(1)–C(1)	103.2(3)	C(6)–P(2)–Ru	117.0(2)
C(3)–P(1)–C(1)	98.1(2)	N(2)–N(1)–Ru	119.4(2)
C(3)–P(1)–C(2)	101.7(2)	N(3)–N(4)–Ru	118.6(2)
C(4)–P(2)–C(5)	103.4(3)	N(1)–N(2)–N(3)	114.2(3)
C(4)–P(2)–C(6)	96.9(2)	N(4)–N(3)–N(2)	114.4(3)
C(5)–P(2)–C(6)	101.3(2)	N(2)–N(1)–C(10)	107.7(3)
N(3)–N(4)–C(20)	107.4(3)		

When R = mes, a second oxidative addition followed by cycloaddition of a further molecule of the azide to the resulting arylimido complex leads to an Ir^{V} intermediate [steps (*iii*) and (*iv*)], which after elimination of two molecules of mesitylene followed by dehydrogenation [steps (*v*)–(*vii*)] gives the final product. It is pertinent to note at this point that bimesityl was not detected in the reaction mixture by spectroscopic methods.

When R = Ph, a second oxidative addition of the NPh group is followed by transfer of the *o*-hydrogen to the metal centre [steps (*iii*)–(*v*)]. Finally, reductive elimination of mesitylene followed by addition of another NPh group and a final azide cycloaddition gives the observed product [steps (*vi*) and (*vii*)]. The observed reactivity difference can be ascribed both to the steric congestion of the flanking *o*-methyl groups, their reluctance to undergo migration and the inertness of aliphatic C–H bonds.

Based on the isoelectronic relationship between carbenes and nitrenes and the recently reported[14] preparation of ruthenium(IV) carbene complexes by interaction of $[RuCl_2(PPh_3)_3]$ with N_2CHPh, the latter acting as a carbene precursor, we applied similar methodology using N_3(mes), which when irradiated in polar solvents can act as a nitrene precursor.

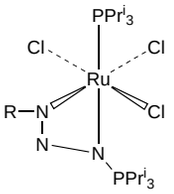

V

Irradiation of a mixture of $[RuCl_2(PPh_3)_3]$ and N_3(mes) in tetrahydrofuran (thf)–methanol in a quartz vessel followed by exchange of PPh_3 with PMe_3 *in situ* gave not the anticipated imido but the tetrazene complex *cis*,*trans*-dichloro(1,4-dimesityltetraza-1,3-diene)bis(trimethylphosphine)ruthenium(II) **4** (structure **IV**). It is diamagnetic and its identity is easily established by analytical and NMR spectroscopic (^{1}H and ^{31}P) data. Its structure has been determined by diffraction methods and is shown in Fig. 4; important bond lengths and angles are in Table 4. The metal geometry is close to octahedral, with the phosphines *trans* to the co-ordinating nitrogens of the bidentate tetrazene ligand. The pseudo C_{2v} symmetry of the $RuCl_2N_2P_2$ molecular core is reflected in the close similarities in the pairs of Ru–Cl, Ru–P and Ru–N bonds and in the N(1)–N(2), N(3)–N(4) bonds. It is pertinent to note that these two bonds are slightly shorter than the central N(2)–N(3) bond, consistent with the formation of the ligand as a $2 \times 2e^{-}$ donor, and the metal as Ru^{II} as shown in structure **IV**. The RuN_4 ring is planar to within 0.09 Å.

The only other products identified in the reaction mixture by ^{31}P NMR spectroscopy are (mes)N=PPh_3 and $[RuCl_2(PMe_3)_4]$, the latter resulting from the interaction of unreacted $[RuCl_2(PPh_3)_3]$ with PMe_3. Compound **4** is thermally stable in the solid state and in solution. It does not react with donors like PMe_3 or pyridine even under forcing conditions (refluxing toluene or UV irradiation). Its formation could have resulted from the insertion of excess azide to a transient ruthenium imido intermediate. Ruthenium(II) imido complexes are known to participate in insertion reactions giving tetrazene complexes.[4a] Attempts to isolate this intermediate by using a deficiency of the azide resulted only in a reduced yield of **4**.

A ruthenium triazenophosphorane complex

Interaction of N_3(mes) with the recently reported ruthenium(IV) complex $[RuH_2Cl_2(PPr^{i}_3)_2]$ gave rise to a paramagnetic triazenophosphorane complex of Ru^{III} *mer*-trichloro(triisopropylphosphine){3-(triisopropylphosphoranediyl)-1-mesityltriaz-1-ene}ruthenium(III) **5**, shown schematically in structure **V**, which was fully characterised by analytical data and a X-ray diffraction study.

The ligand $RNNNPR'_3$ (R = aryl, R′ = alkyl or aryl) originally named by Staudinger as phosphazide is an intermediate in reactions between organic azides and phosphines. It is usually unstable at room temperature unless the azide carries electron-withdrawing substituents. A discussion of these intermediates together with recent advances in the Staudinger reaction has appeared.[15] Triazenophosphorane is related to the diazenylimido ligand (*e.g.* end-on co-ordinated organic azide) recently reported by Proulx and Bergman[16] and Cummings and co-workers.[17]

To our knowledge the only other structurally characterised example of a triazenophosphorane complex is $[W(CO)_2Br(tolNNNPPh_3)]$ (tol = *p*-tolyl, C_6H_4Me-4) reported by Hillhouse *et al.*[18]

The crystal structure of complex **5** is shown in Fig. 5; important bond lengths and angles are in Table 5. The molecule has a distorted octahedral geometry which is *mer* with respect to the three chlorine atoms. The Ru–N bonds, which are *trans* to P and Cl are remarkably similar in length, as are the three Ru–Cl bonds. In the tungsten complex mentioned above,[18] the

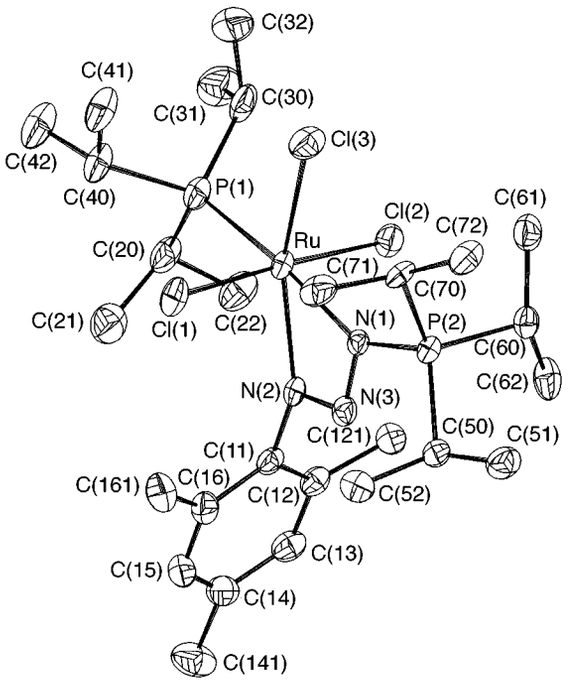

Fig. 5 The structure of compound **5**

Table 5 Bond lengths (Å) and angles (°) for compound **5**

Ru–N(1)	2.151(4)	Ru–Cl(1)	2.349(2)
Ru–N(2)	2.150(5)	Ru–Cl(2)	2.348(2)
Ru–N(3)	2.671(5)	Ru–Cl(3)	2.341(2)
Ru–P(1)	2.367(2)	N(1)–P(2)	1.672(5)
N(1)–N(3)	1.361(6)	N(2)–N(3)	1.286(6)
P(1)–C(20)	1.839(7)	P(2)–C(50)	1.813(6)
P(1)–C(30)	1.858(7)	P(2)–C(60)	1.814(6)
P(1)–C(40)	1.854(6)	P(2)–C(70)	1.797(5)
N(1)–Ru–N(2)	58.8(2)	N(1)–Ru–P(1)	173.22(14)
N(1)–Ru–Cl(1)	89.35(12)	N(2)–Ru–P(1)	114.47(14)
N(1)–Ru–Cl(2)	90.00(12)	N(1)–Ru–N(3)	30.4(2)
N(1)–Ru–Cl(3)	98.77(14)	N(2)–Ru–N(3)	28.4(2)
N(2)–Ru–Cl(1)	88.89(13)	Cl(1)–Ru–Cl(2)	176.68(7)
N(2)–Ru–Cl(2)	87.98(13)	Cl(3)–Ru–Cl(1)	92.90(6)
N(2)–Ru–Cl(3)	157.50(13)	Cl(3)–Ru–Cl(2)	90.41(6)
Cl(1)–Ru–P(1)	91.39(6)	Cl(1)–Ru–N(3)	89.33(11)
Cl(2)–Ru–P(1)	88.88(6)	Cl(2)–Ru–N(3)	88.45(11)
Cl(3)–Ru–P(1)	87.93(6)	Cl(3)–Ru–N(3)	129.15(12)
N(3)–N(1)–Ru	96.4(3)	N(3)–N(1)–P(2)	115.2(4)
N(3)–N(2)–Ru	99.0(4)	N(2)–N(3)–N(1)	105.8(4)

W–N distances are different, probably reflecting the occupancy of a normal and a capping site in a capped octahedral coordination geometry. Bond lengths in the triazenophosphorane of **5** are consistent with its formulation as $RN{=}N{-}N{=}PR_3$. The Ru atom is 0.039 Å out of the N_3 plane.

The reduction of ruthenium during the present transformation combined with the fact that less than 50% yields are obtained is indicative of a disproportionation reaction as a productive step. No other products have been isolated.

A ruthenium amide complex

The compound *trans*-$[RuCl_2(PMe_3)_4]$ is relatively inert in substitution reactions of chloride by anionic amides.[19,20] However, interaction with 2 equivalents of $Li[NH(C_6H_3Pr^i_2\text{-}2,6)]$ in refluxing dibutyl ether gave after work-up crystalline allyl–amide (2-isopropyl-6-yloallylphenylamido)tris(trimethylphosphine)ruthenium(II) **6**, which contains a novel dianionic hybrid ligand. Complex **6** was adequately characterised by spectroscopic (NMR) and analytical methods. The ^{31}P NMR spectrum consists of an A_2B pattern supporting the presence of two groups of magnetically inequivalent phosphorus nuclei.

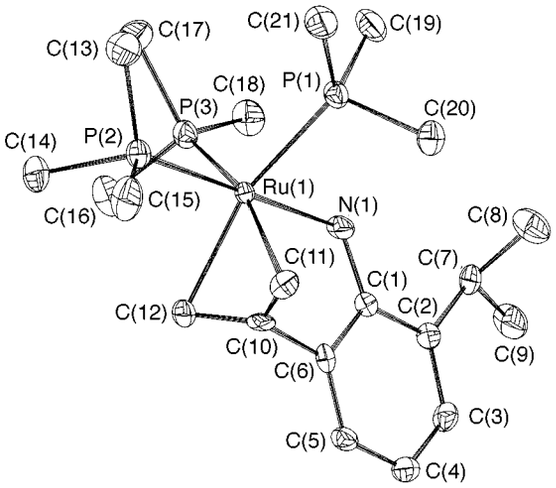

Fig. 6 The structure of the ruthenium amide **6**

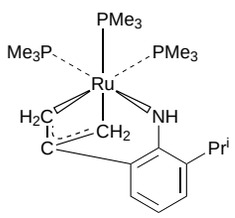

VI

Table 6 Bond lengths (Å) and angles (°) for compound **6**

Ru(1)–N(1)	2.138(3)	Ru(2)–N(2)	2.137(3)
Ru(1)–P(1)	2.3206(11)	Ru(2)–P(4)	2.2934(12)
Ru(1)–P(2)	2.3146(12)	Ru(2)–P(5)	2.3035(12)
Ru(1)–P(3)	2.3133(13)	Ru(2)–P(6)	2.3112(11)
Ru(1)–C(10)	2.198(3)	Ru(2)–C(31)	2.197(3)
Ru(1)–C(11)	2.281(4)	Ru(2)–C(32)	2.302(4)
Ru(1)–C(12)	2.258(4)	Ru(2)–C(33)	2.242(4)
N(1)–C(1)	1.350(4)	N(2)–C(22)	1.349(4)
N(1)–Ru(1)–C(10)	75.26(12)	N(2)–Ru(2)–C(31)	74.79(11)
N(1)–Ru(1)–C(11)	91.35(13)	N(2)–Ru(2)–C(32)	93.28(13)
N(1)–Ru(1)–C(12)	93.07(13)	N(2)–Ru(2)–C(33)	90.63(14)
N(1)–Ru(1)–P(1)	82.08(9)	N(2)–Ru(2)–P(4)	88.57(9)
N(1)–Ru(1)–P(2)	178.19(9)	N(2)–Ru(2)–P(5)	175.16(9)
N(1)–Ru(1)–P(3)	86.81(9)	N(2)–Ru(2)–P(6)	84.03(9)
P(2)–Ru(1)–P(1)	98.62(4)	P(4)–Ru(2)–P(5)	95.39(5)
P(3)–Ru(1)–P(1)	101.73(5)	P(4)–Ru(2)–P(6)	100.22(4)
P(3)–Ru(1)–P(2)	91.42(5)	P(5)–Ru(2)–P(6)	92.50(5)
C(10)–Ru(1)–C(11)	36.88(13)	C(31)–Ru(2)–C(32)	35.79(13)
C(10)–Ru(1)–C(12)	36.57(13)	C(31)–Ru(2)–C(33)	37.64(13)
C(12)–Ru(1)–C(11)	65.73(14)	C(33)–Ru(2)–C(32)	65.5(2)

Furthermore, the magnitude of $^2J_{P\text{–}P}$ (31 Hz) indicates *cis* arrangement of the coupled nuclei. In the ^{1}H NMR spectrum the presence of the allyl group is evidenced by the appearance of an A_2B_2 pattern which can be assigned to the magnetically inequivalent *exo* and *endo* protons of the η^3-$CH_2(CR')CH_2$ ($R' = NHC_6H_3Pr^i$) group. Complex **6** is non-fluxional in $[^2H_8]$toluene between −50 and +80 °C.

The structure of **6**, shown schematically in structure **VI** has been determined by X-ray diffraction methods. The structure contains two crystallographically independent molecules which are essentially equivalent. A diagram of one molecule is shown in Fig. 6; important bond lengths and angles are given in Table 6. The metal geometry is distorted octahedral, with the allyl functions assumed to occupy two *cis* sites and the phosphines have a *fac* arrangement. Notwithstanding the site differences, *i.e. trans* to N or allyl carbons, the Ru–P distances are all very similar.

A plausible mechanism accounting for the formation of **6** is shown in Scheme 3 and involves substitution of the first

Table 7 Analytical and physical data for new compounds

Compound	Colour	M.p./°C	Analysis (%) [a] C	H	N
1	Blue	143–145 (decomp.)	59.1 (58.9)	5.8 (5.5)	9.2 (9.5)
3	Blue-grey	171–173	*b*		
4	Orange-red	222–225	42.3 (42.7)	5.7 (5.9)	8.1 (8.3)
5	Orange	205 (decomp.)	46.5 (47.0)	7.7 (7.7)	5.9 (6.1)
6	Yellow	165 (decomp.)	49.8 (50.0)	8.3 (8.5)	2.5 (2.8)

[a] Calculated values in parentheses. [b] No reliable analytical data available, for accurate mass spectra see below.

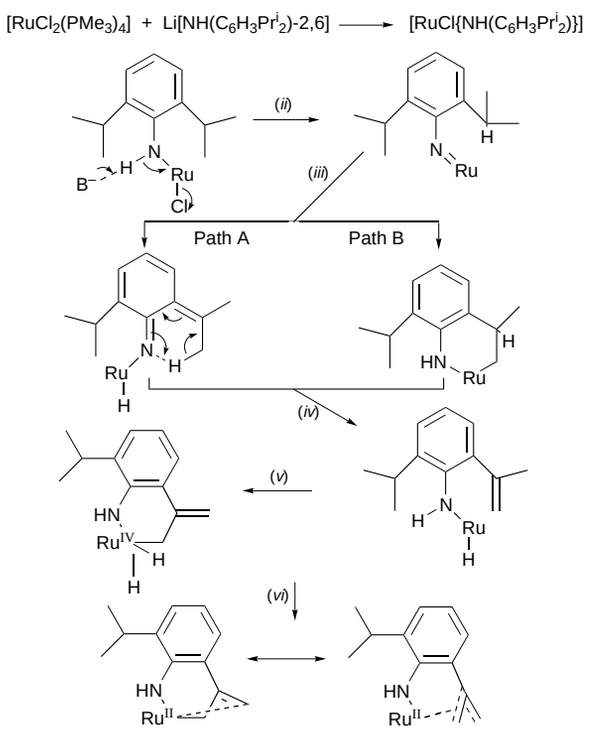

Scheme 3 Proposed mechanism for the formation of the ruthenium amide **6**: (*i*) -LiCl; (*ii*) -Cl^-, -B, -H; (*iii*) pericyclic H migration (path A) or C–H bond addition (path B); (*iv*) β-hydride elimination; (*v*) oxidative addition; (*vi*) -H_2

chloride by the amide group and base-induced dehydrohalogenation [steps (*i*) and (*ii*)] to generate the ruthenium imido complex as a key intermediate. Formal dehydrogenation of one of the neighbouring *ortho* isopropyl groups can then occur either *via* a series of two consecutive pericyclic hydrogen migrations (path A) or *via* the cyclometallated intermediate formed by addition of a C–H bond of the methyl group across the ruthenium imido bond [step (*iii*), path B] and subsequent β-hydride elimination [step (*iv*)]. Oxidative addition of one of the C–H bonds of the activated allylic methyl group [step (*v*)] and a final dihydrogen reductive elimination [step (*vi*)] can then account for the observed product.

Experimental

Analyses were by Imperial College microanalytical laboratory. All operations were carried out under purified Ar or N_2, under vacuum or in a Vacuum Atmospheres glove-box. General techniques have been described previously.[21] The NMR spectroscopic data were obtained on a JEOL EX-270, a Bruker Avance DRX-300 or a Varian VRX-400 spectrometer operating at 270, 300 or 400 MHz (^{1}H), respectively and referenced to the residual ^{1}H impurity in the solvent (δ 7.15, C_6D_6; 7.26, $CDCl_3$, 5.3, CD_2Cl_2); ^{31}P spectra were referenced externally relative to H_3PO_4. Mass spectra were recorded using VG-7070E and VG Autospec spectrometers. Commercial chemicals were from Aldrich and Avocado. The light petroleum used had b.p. 40–60 °C.

The following starting materials were prepared as referenced: N_3(mes),[22] N_3Ph,[23] Ir(mes)$_3$,[5] [$RuCl_2(PPh_3)_3$],[24] *trans*-[$RuCl_2(PMe_3)_4$],[25] [$RuH_2Cl_2(PPr^i_3)_2$];[26] the compound Li[NH($C_6H_3Pr^i_2$-2,6)] was prepared by interaction of distilled aniline with the stoichiometric amount of $LiBu^n$ in light petroleum.

Photolysis were carried out in a quartz apparatus using a 125 W medium pressure Hg lamp.

Analytical and physical data for the new compounds are given in Table 7.

Compound 1

To a stirred solution of Ir(mes)$_3$ (0.14 g, 0.26 mmol) in diethyl ether (15 cm^3) was added a solution of N_3(mes) (0.165 g, 1.02 mmol) in diethyl ether (15 cm^3). After stirring the reaction mixture at room temperature for 8 h, the volatiles were removed under vacuum and the residue was extracted with light petroleum (2 × 10 cm^3). Removal of light petroleum under reduced pressure gave the crude product, which was further purified by column chromatography (neutral alumina, activity I, the elution was started using hexane followed by hexane to which CH_2Cl_2 was added in 6% steps up to 50% CH_2Cl_2). The dark blue air-stable paste obtained by evaporation of volatiles under reduced pressure which is a CH_2Cl_2 solvate of **1** (by NMR spectroscopy) was crystallised from diethyl ether, by slow evaporation to give dark blue crystals of **1**. Yield: 0.125 g, 67%. NMR (C_6D_6): ^{1}H, δ 7.05, 7.02, 6.72, 6.57, 6.50, 6.39, 6.37, 6.03 (s, 1 H each, aromatic), 5.56 (d, 1 H, C*H*=CH, *J* = 9.4), 4.90 (d, 1 H, CH=C*H*, *J* = 9.4 Hz), 2.88, 2.21, 2.15, 2.08, 2.06, 2.05, 1.93, 1.90, 1.58 and 1.29 (s, 3 H each, CH_3).

Compound 2

A solution of a crude CH_2Cl_2 solvate of **1** in toluene (0.03 g in 10 cm^3) in a sealed tube was heated to 140 °C for 4 h. After cooling to room temperature and removal of volatiles under vacuum, the residue was purified by column chromatography on neutral alumina (activity I). The elution was started with hexane followed by hexane to which diethyl ether was added in 10% steps up to 50% diethyl ether. Evaporation of volatiles from the combined eluents gave **2** as a dark grey-blue solid. Yield: 0.005–0.01 g, 20–40%. X-Ray quality crystals were obtained by slow evaporation of diethyl ether solutions. NMR (CD_2Cl_2): ^{1}H, δ 12.70 (s, 1 H, NH), 7.25, 7.20, 6.87, 6.62 (s, 1 H each, aromatic), 6.81 (br s, 2 H aromatic), 5.88 (d, 1 H, C*H*=CH, *J* = 8.7), 5.68 (d, 1 H, CH=CH, *J* = 8.7 Hz), 2.34, 2.24, 2.15, 1.94, 1.84, 1.60 and 1.27 (s, 3 H each, CH_3).

Compound 3

To a stirred solution of Ir(mes)$_3$ (0.1 g, 0.18 mmol) in diethyl ether (20 cm^3) was added a solution of N_3Ph in hexane (4.7 cm^3 of 0.14 M). The reaction mixture was stirred vigorously at room temperature for 2 d. After removal of the volatiles under vacuum the crude air stable product was purified by column chromatography on neutral alumina, activity I. The elution was started using light petroleum, followed by light petroleum to

Table 8 Crystal data and structure refinement details for compounds **1**–**6**

	1	**2**	**3**	**4**	**5**	**6**
Formula	$[C_{36}H_{40}IrN_5][C_2H_5O]_{0.5}$	$C_{27}H_{29}ClIrN_2$	$C_{42}H_{41}IrN_6$	$C_{24}H_{40}Cl_2N_4P_2Ru$	$C_{30}H_{53}Cl_3N_3P_2Ru$	$C_{42}H_{84}N_2P_6Ru_2$
M_r	750.94	609.17	822.01	618.51	725.14	1 005.07
Crystal system	Triclinic	Monoclinic	Monoclinic	Trigonal	Monoclinic	Monoclinic
Space group	$P\bar{1}$	$P2_1/n$	$C2/c$	$R3c$	$P2_1/c$	$P2_1/n$
a/Å	11.022(4)	11.464(4)	28.494(6)	27.222(4)	9.9780(10)	17.797(7)
b/Å	11.871(3)	12.1730(10)	19.187(4)	27.222(4)	10.798(3)	11.726(2)
c/Å	13.493(3)	16.887(3)	15.604(3)	20.426(4)	33.685(2)	25.3200(10)
α/°	74.76(5)			90		
β/°	76.45(4)	90.627(11)	112.34(3)	90	94.79(2)	110.00(4)
γ/°	87.19(2)			120		
U/Å^3	1655.8(8)	2356.5(9)	7891(3)	13 109(4)	3616.6(11)	4965(2)
Z	2	4	8	18	4	4
D_c/Mg m^{-3}	1.506	1.717	1.384	1.410	1.332	1.345
F(000)	752	1196	3296	5760	1516	2112
Crystal size/mm	0.18 × 0.18 × 0.12	0.12 × 0.15 × 0.13	0.18 × 0.16 × 0.05	0.17 × 0.12 × 0.09	0.13 × 0.15 × 0.15	0.17 × 0.28 × 0.12
μ(Mo-Kα)/mm^{-1}	3.926	5.600	3.419	0.810	0.733	0.783
T/K	150	150	150	150	150	150
Reflections collected	6486	8677	31 834	17 890	13 581	19 723
Independent reflections (R_{int})	4624 (0.0804)	3454 (0.0577)	5836 (0.0607)	4092 (0.0654)	5235 (0.0943)	7234 (0.0607)
Maximum, minimum correction factors	1.285, 0.811	1.133, 0.866	1.100, 0.998	1.044, 0.919	1.138, 0.700	1.097, 0.914
Data, restraints, parameters	4622, 18, 406	3452, 0, 287	5836, 0, 448	4090, 1, 310	5228, 0, 394	7230, 0, 805
Goodness of fit, F^2	1.046	0.639	0.871	0.868	0.827	0.789
Final $R1$, $wR2$* [$I > 2\sigma(I)$]	0.0582, 0.1429	0.0277, 0.0519	0.0332, 0.0690	0.0247, 0.0514	0.0462, 0.0843	0.0280, 0.0536
(all data)	0.0691, 0.1550	0.0523, 0.0547	0.0668, 0.0729	0.0313, 0.0627	0.0946, 0.1043	0.0435, 0.0712
Largest difference peak and hole/e Å^{-3}	2.400, −1.601	1.156, −0.561	1.450, −0.679	0.293, −0.316	0.637, −0.350	0.470, −0.438

* Goodness of fit, $S = [\Sigma w(F_o^2 - F_c^2)^2/(n-p)]^{\frac{1}{2}}$ where n = number of reflections and p = total number of parameters; $R1 = \Sigma|F_o - F_c|/\Sigma F_o$; $wR2 = [\Sigma(F_o^2 - F_c^2)^2/\Sigma w(F_o^2)^2]^{\frac{1}{2}}$ where $w = 1/[\sigma^2(F_o)^2 + (xP)^2]$ with $x = 0.0759$, 0.0000, 0.0193, 0.0140, 0.0183 and 0.0000 for **1**, **2**, **3**, **4**, **5** and **6** and $P = [\max(F_o^2) + (2F_c^2)]/3$.

which diethyl ether was added in steps of 4% up to 16% diethyl ether. The dark blue solid obtained after evaporation of volatiles from the combined eluents was further purified by slow evaporation of light petroleum solutions. Yield: 0.0218 g, 14%. Accurate chemical ionization (CI) mass spectrum: *m*/*z* 822.3052 (Calc. for $C_{42}H_{41}IrN_6$ 822.3022) and 794.2967 ($M^+ - N_2$). NMR (C_6D_6): ^{1}H, δ 7.60–6.51 (m, 21 H, aromatic), 6.47, 6.16 (s, 1 H each, $C_6H_2Me_3$), 2.23, 2.11, 2.05, 1.67, 1.54, 0.78 (s, 3 H each, $C_6H_2Me_3$).

Compound 4

To a solution of $[RuCl_2(PPh_3)_3]$ (0.48 g, 0.5 mmol) in thf–methanol (20 cm^3, 2:1) at room temperature was added a solution of N_3(mes) in thf (0.17 g, 1.0 mmol in 10 cm^3) and the mixture was photolysed for 2 h. During this time N_2 evolution was observed. After addition of more N_3(mes) (0.08 g, 0.5 mmol) photolysis was continued for 2 h. To the yellow-brown reaction mixture obtained was added PMe_3 (0.4 cm^3, excess) and stirring continued for 4 h. Evaporation of volatiles under reduced pressure, extraction of the residue with light petroleum until the extracts were colourless (*ca.* 4 × 20 cm^3), followed by concentration of the filtered extracts to *ca.* 20 cm^3 and standing at room temperature for 8 h gave orange-red prisms. Yield: 0.17 g, 55%. NMR (C_6D_6): ^{1}H, δ 6.65 (s, 4 H, $C_6H_2Me_3$), 2.32 (s, 12 H, *o*-$Me_2C_6H_2Me$), 2.18 (s, 6 H, *p*-$MeC_6H_2Me_2$) and 0.98 (filled-in d, 18 H, PMe_3); ^{31}P, δ −17.7 (s).

Compound 5

To a solution of $[RuH_2Cl_2(PPr^i_3)_2]$ in thf (0.49 g, 1 mmol in 30 cm^3) at room temperature was added dropwise a solution of N_3(mes) in the same solvent (0.32 g, 2 mmol in 10 cm^3). The colour of the reaction mixture changed successively from yellow-orange to green-yellow to orange within 5 min. Stirring was continued for *ca.* 3 h. At this time ^{31}P NMR spectra of aliquots showed complete consumption of the starting material. After removal of volatiles under vacuum, washing of the orange residue with light petroleum, extraction in toluene (3 × 15 cm^3), concentration of the toluene extracts to *ca.* 10 cm^3 and cooling (−20 °C) gave orange crystals. Yield: 0.31 g, 45%.

Compound 6

A mixture of *trans*-$[RuCl_2(PMe_3)_4]$ (0.48 g, 1 mmol) and $Li[NH(C_6H_3Pr^i_2\text{-}2,6)]$ in di-*n*-butyl ether (20 cm^3) was refluxed for *ca.* 4 h. Removal of volatiles at 70 °C under vacuum, extraction of the yellow residue with light petroleum (30 cm^3), filtration and concentration of the extracts to 5 cm^3 and cooling (−20 °C) for 2 d gave yellow very air-sensitive crystals. Yield: 0.2 g, 40%. NMR (C_6D_6): ^{1}H, δ 7.40 (d, 1 H, aromatic), 7.02 (d, 1 H, aromatic), 6.52 (t, 1 H, aromatic), 3.4 (s br, 1 H, NH), 2.83 (spt, 1 H, CH_3CHCH_3), 1.75 and 1.72 (d, 2 H each, CH_2CCH_2) 1.32 (d, 6 H, CH_3CHCH_3), 1.15 (d, 18 H, PMe_3) and 0.62 (d, 9 H, PMe_3); ^{31}P, δ 3.210 (t) and 0.30 (d), $^2J_{P-P}$ = 31 Hz.

Crystallography

X-Ray data for compounds **1**–**6** were collected at low temperature; details are listed in Table 8. A FAST TV area detector diffractometer with Mo-Kα radiation (λ = 0.71 069 Å) was employed, as previously described.[27] The structure of compound **5** was solved using the PATT instruction of SHELXS 86,[28] those of **1**–**4** and **6** *via* direct method procedures of the same program. The structures were refined by full-matrix least squares on F_o^2, using the program SHELXL 93.[29] Corrections for absorption were applied using the DIFABS program[30] with maximum and minimum correction factors listed in Table 8. The non-hydrogen atoms were refined with anisotropic thermal parameters. All of the hydrogen atoms in compounds **1**–**5** were included in idealised positions, except for the olefin protons of **1** which were experimentally located. All protons in **6** were located experimentally. In the crystal structure of **1** a disordered solvent molecule (diethyl ether) appeared to be present at partial occupancy in a cavity around 0.5, 0, 0. It was not possible to model this to a chemically sensible structure but partial atoms were included coincident with the three major peaks present in the difference map. Refinement indicates an occupancy of about 0.5.

CCDC reference number 186/630.

Acknowledgements

We thank Professor W. B. Motherwell (University College London) for helpful discussions and interest. A. A. D. and S. M. C. are indebted to the Wilkinson Trust for financial support. Partial support by EPSRC is also acknowledged (to R. S. H.-M.).

References

1 W. A. Nugent and J. M. Mayer, *Metal-Ligand Multiple Bonds*, Wiley, New York, 1988; D. E. Wigley, *Prog. Inorg. Chem.*, 1994, **42**, 239.
2 D. S. Glueck, J. Wu, F. J. Hollander and R. G. Bergman, *J. Am. Chem. Soc.*, 1991, **113**, 2041; D. A. Dobbs and R. G. Bergman, *Organometallics*, 1994, **13**, 4594.
3 A. K. Burrell and A. J. Steedman, *J. Chem. Soc., Chem. Commun.*, 1995, 2109.
4 (*a*) A. A. Danopoulos, G. Wilkinson, B. Hussain-Bates and M. B. Hursthouse, *J. Chem. Soc., Dalton Trans.*, 1996, 3771; (*b*) A. A. Danopoulos, G. Wilkinson, B. Hussain-Bates and M. B. Hursthouse, *Polyhedron*, 1992, **11**, 2961.
5 R. S. Hay-Motherwell, G. Wilkinson, B. Hussain-Bates and M. B. Hursthouse, *J. Chem. Soc., Dalton Trans.*, 1992, 3477.
6 R. S. Hay-Motherwell, G. Wilkinson, B. Hussain-Bates and M. B. Hursthouse, *Polyhedron*, 1993, **12**, 2009.
7 F. A. Cotton and G. Wilkinson, *Advanced Inorganic Chemistry*, Wiley, New York, 5th edn., 1988, p. 916; X.-L. Luo and R. H. Crabtree, *J. Am. Chem. Soc.*, 1989, **111**, 2527; R. S. Tanke and R. H. Crabtree, *Organometallics*, 1991, **10**, 615.
8 M. D. Fryzuk, P. A. McNeil and S. Rettig, *Organometallics*, 1986, **5**, 2469.
9 M. Rahim and K. J. Ahmet, *Organometallics*, 1994, **13**, 1751.
10 P. A. S. Smith, in *Azides and Nitrenes, Reactivity and Utility*, ed. E. F. V. Scriven, Academic Press, Orlando, 1984, p. 104.
11 M. S. Platz, *Acc. Chem. Res.*, 1995, **28**, 487.
12 G. A. Miller, S. W. Lee and W. C. Trogler, *Organometallics*, 1989, **8**, 738.
13 P. T. Matsunaga, C. R. Hess and G. L. Hillhouse, *J. Am. Chem. Soc.*, 1994, **116**, 3665.
14 P. Schwab, R. H. Grubbs and J. W. Ziller, *J. Am. Chem. Soc.*, 1996, **118**, 100.
15 Y. G. Godolobov and L. F. Kasukhin, *Tetrahedron*, 1992, **48**, 1353.
16 G. Proulx and R. G. Bergman, *J. Am. Chem. Soc.*, 1995, **117**, 6382.
17 M. G. Fickes, W. H. Davis and C. C. Cummings, *J. Am. Chem. Soc.*, 1995, **117**, 6384.
18 G. L. Hillhouse, G. V. Goeden and B. L. Haymore, *Inorg. Chem.*, 1982, **21**, 2064.
19 V. V. Mainz and R.A. Andersen, *Organometallics*, 1984, **3**, 675.
20 D. M. Hankin, A. A. Danopoulos, G. Wilkinson, T. K. N. Sweet and M. B. Hursthouse, *J. Chem. Soc., Dalton Trans.*, 1996, 4063 and refs. therein.
21 A. A. Danopoulos, A. C. C. Wong, G. Wilkinson, B. Hussain-Bates and M. B. Hursthouse, *J. Chem. Soc., Dalton Trans.*, 1990, 315.
22 K. Baum, *J. Org. Chem.*, 1968, **33**, 4333.
23 R. O. Lindsay and C. F. H. Allen, *Org. Synth.*, 1955, **Coll. Vol. 3**, 710.
24 T. A. Stephenson and G. Wilkinson, *J. Inorg. Nucl. Chem.*, 1966, **28**, 945.
25 H. Schmidbaur and G. Blaschke, *Z. Naturforsch., Teil B*, 1980, **35**, 584.
26 C. Grunwald, O. Gevert, J. Wolf, P. Gonzalez-Herrero and H. Werner, *Organometallics*, 1996, **15**, 1960.
27 A. A. Danopoulos, G. Wilkinson, B. Hussain-Bates and M. B. Hursthouse, *J. Chem. Soc., Dalton Trans.*, 1991, 1855.
28 G. M. Sheldrick, SHELXS 86, *Acta Crystallogr., Sect. A*, 1990, **46**, 467.
29 G. M. Sheldrick, SHELXL 93, Program for Crystal Structure Refinement, University of Göttingen, 1993.
30 N. P. C. Walker and D. Stuart, *Acta Crystallogr., Sect. A*, 1983, **39**, 158 (adapted for FAST geometry by A. Karaulov, University of Wales Cardiff, 1991).

Received 2*nd May* 1997; *Paper* 7/03028B